Bitter Sweet Symphony: the impact of sugars on autoimmunity

Kissel, T.

N-linked glycans attached to the immunoglobulin variable domain affect the recruitment of complement

Theresa Kissel, Sanne van de Bovenkamp, Hugo J. van Dooren, Astrid S. Brehler, Joanneke C. Kwekkeboom, Eva M. Stork, Carolien Koeleman, Manfred Wuhrer, Tom W.J. Huizinga, Hans U. Scherer, Leendert A. Trouw, René E.M. Toes

Manuscript in preparation

Abstract

Recruitment and activation of the complement system represents an important effector mechanism of (auto)antibodies. Previous studies have shown that the autoantibodies characteristic of Rheumatoid Arthritis (RA), anti-citrullinated protein antibodies (ACPAs), are capable of activating the classical and alternative complement cascade. ACPA immunoglobulin gamma (IgG) are extensively N-linked glycosylated in their variable domains. In contrast to the role of the evolutionary conserved Fc glycan at position 297, the influence of variable domain glycans (VDGs) on the biological function of antibodies remains to be elucidated.

In this study, we investigated the effects of VDGs on complement activation using patient-derived monoclonal ACPA IgG with and without naturally occurring N-linked glycans in the variable domain. We show that monoclonal ACPA IgG activated the classical and alternative complement cascade in a dose-dependent manner consistent with the results observed for polyclonal ACPA. Interestingly, the presence of VDGs resulted in impaired initiation of the classical but not the alternative complement pathway. This was explained by reduced C1q binding and decreased subsequent C4 and C3c deposition, especially for ACPA IgG carrying a high amount of VDGs. The decreased binding of C1q was explained by the reduced ability of VDG-bearing IgG to hexamerize, which is crucial for IgG to interact efficiently with C1q, rather than by differences in antigen binding.

Collectively, these results show that glycans attached to the variable domain of autoantibodies inhibit initiation of the classical complement pathway and reveal a novel mechanism that affects the ability of antibodies to recruit a key immune effector mechanism. These data suggest that glycan modifications in the variable domain could potentially be employed to influence the complement-activating potential of IgG (auto)antibodies.

Introduction

The complement system is an important innate defense cascade that can mediate a plethora of functions in the host defense against invading pathogens and protection against autoimmunity[1-3]. Complement can be activated via the classical, the alternative and the lectin pathway[4]. The classical pathway is initiated by binding of C1q to antibody-antigen immune complexes, preferentially hexamers, and often assessed by circulating levels of activated C4. The lectin pathway is triggered by mannose-binding lectin (MBL) or ficolins whereas the alternative pathway is initiated by an "autoactivation" of the complement factor C3. Central to complement activation is the formation of C3 convertases (C3c) that cleave C3 to biologically active complement fragments resulting in the recruitment and activation of immune cells as well as cell lysis after formation of the membrane attack complex. Importantly, the induction of complement is tightly regulated and aberrant activation can lead to severe tissue damage. Complement is likely also playing a role in human autoimmune diseases as complement inhibition has been proven effective[5,6] and complement activation products are often found at sites of inflammation. For example, in the synovial fluid of RA patients elevated levels of complement activation products such as SC5b-9, Bb or C1q-C4 complexes are readily detected[7-9]. Similarly, complement deposits can be visualized in the synovial membrane[10], indicating local complement activation in the synovium of RA patients.

The prominent autoimmune disease RA is characterized by autoantibodies directed against citrullinated residues expressed by proteins, termed anti-citrullinated protein antibodies (ACPAs). ACPAs have a remarkably specificity for RA, can be present several years before the actual onset of RA and their presence is associated with a worsened disease course[11-14]. Recent studies have shown that ACPA are capable of activating both the classical and alternative complement cascade in an antigen-dependent in vitro assay[15] suggesting a potential contribution to disease pathogenesis via the complement system. As an integral feature, ACPA IgG harbor glycans not only at the evolutionary conserved N-linked glycosylation site at position 297 in the Fc domain, but also in the variable domains of the heavy and light chains (V_H and V_L, respectively). Structural analysis revealed that ACPA IgG VDGs are predominantly fully processed diantennary complex type glycans presenting a bisecting *N*-acetylglucosamine and two terminal sialic acids[16]. Intriguingly, VDGs are present on more than 90% of the RA-specific autoantibodies[16] and their introduction has been reported to be predictive for disease development with increasing levels towards RA-onset[17-19]. Recently, it has been suggested that the abundant introduction of N-glycosylation sites in the hypervariable regions of ACPA IgG molecules[20,21] likely provides a selective advantage to citrullinated protein-reactive B cells[22].

Nevertheless, VDGs are not unique to ACPA, but also present on conventional IgG molecules albeit at a lower level of approximately 15%[23]. Interestingly elevated levels of VDGs were also found on (auto)antibodies from ANCA-associated vasculitis (AAV)-patients (anti-MPO, anti-

PR3, anti-GBM)[24], primary Sjorgen's syndrome (pSS), multiple sclerosis (MS) or systemic lupus erythematosus (SLE) patients[25,26]. VDGs were also found to be present in monoclonal muscle-specific kinase (MuSK) autoantibodies, suggesting a potential role for myasthenia gravis[27,28]. In addition, glycans are frequently presented in the variable domains of anti-drug antibodies that emerge in patients treated with adalimumab or infliximab[29]. Thus, increased variable domain glycosylation appears to be a common feature of several (autoreactive) B-cell responses potentially triggered by chronic, systemic antigen exposure and may pursue important immunomodulatory functions.

It is well established that the conserved N-linked glycans in the IgG Fc domain can modulate immune effector functions by interacting with the complement system[30-32]. The composition of the Fc glycans is variable and it has been reported that Fc galactosylation and sialylation affect binding to C1q and, thereby, complement-dependent cytotoxicity (CDC). For Fc galactosylation enhanced binding to C1q has been reported[30,33], whereas conflicting data have been observed for IgG sialylation[30,34,35]. Recently, the mechanism by which Fc galactosylation affects complement activation has been elucidated, as it has been shown that hypergalactosylation enhances the potential of IgG to form hexameric structures, which is a pre-requisite for efficient C1q binding and subsequent CDC, rather than directly impacting on the affinity/avidity of individual Fc tails to C1q[35].

Given the importance of IgG-Fc N-linked glycans on immune effector functions and the abundant occurrence of glycans in the variable domains on ACPAs, we now wished to determine the potential impact of VDGs on complement activation. To study this, we created a set of glycoengineered monoclonal antibodies (mAbs) expressing N-linked glycans in the variable domain and analyzed their ability to facilitate complement binding and activation. Furthermore, we assessed the impact of VDGs on the propensity of IgG molecules to form hexamer structures, accompanied by efficient C1q binding, by generating RGY triple mutants (E345R, E430G and S440Y).

Results

Glycoengineered human monoclonal antibodies with and without N-linked variable domain glycans

To investigate the effect of antibody VDGs on complement activation, we generated monoclonal ACPA IgG, derived from B-cell receptor sequences obtained from RA patients. These mAbs harbor 2 to 4 naturally occurring N-linked glycan sites in the heavy chain (HC) and light chain (LC) variable regions (Figure 1A). To produce non-variable domain glycosylated monoclonal antibody (mAb) counterparts, the N-linked glycan motifs were mutated back to the respective

germline sequences (Table S1). The integrity of the wild-type (WT, i.e. the sequence with N-glycosylation sites), and non-glycosylated (NG) mAbs (lacking the VDGs) was verified by gel electrophoresis (Figure 1B). The shift in the apparent molecular weight between both variants indicates the presence of glycans and was in line with an increasing number of glycan-sites (7E4 < 3F3 < 2G9). As indicated by the gel bands depicted in figure 1B, all glycosylation sites in the mAb HC and LC were occupied by a glycan, except for a fraction of the ACPA 2G9 HC and LC glycan sites which were only partially used. Next to the ACPA IgG, we further cloned and expressed an anti-tetanus toxoid (anti-TT) IgG mAb (D2) with and without its natural LC N-glycan site to determine whether the findings generated were specific for ACPAs or likely reflect a general effect of VDGs (Figure S1A). As for monoclonal ACPA IgG, also the sequence of the anti-TT mAb was derived from sorted antigen-specific B cells obtained from RA patients.

Since ACPA VDGs mainly consist of diantennary glycans harboring terminal sialic acids, we produced glycoengineered (+ge) variants of the mAbs (see Materials and Methods)[16]. To investigate the effect of different glycan compositions, the mAb 7E4 was generated in the presence and absence of glycoengineering. Different Fc-glycan profiles for the mAb variants were observed as determined by liquid chromatography coupled to mass spectrometry (LC-MS) with an increased percentage of galactosylation, sialylation and bisection for the glycoengineered molecules (Figure 1, C and E). Importantly, the Fc-glycan profiles between the WT and NG variant of each set of mAbs were similar when generated under the same conditions (Figure 1 and S1). Glycan analysis after total glycan release revealed a dominating complex-type, bisected and disialylated VDG profile (m/z = 2651) after glycoengineering (Figure 1F and S2). Consequently specific glycoengineering of Freestyle™ 293-F cells enables the generation of mAbs with complex-type disialylated VDG-glycan profiles similar to those obtained on secreted autoantibodies from RA patients. Together, we generated and characterized four different mAbs with VDGs and their non-VDG containing counterparts to address the functional relevance of antibody VDGs on complement activation.

IgG variable domain glycosylation hampers the activation of the classical complement pathway

To assess whether the presence of VDGs affects the complement cascade, we determined the ability of the different mAb IgG variants to activate the classical or alternative complement pathway. Because antigen binding is a pre-requisite for complement activation, ACPA IgG were first incubated on a plate coated with the antigen cyclic citrullinated peptide 2 (CCP2) (Figure 2A). To obtain similar binding for the WT and NG antibody variants (Figure 2B) we adjusted antigen-coating for the 7E4 mAbs (see Materials and Methods). No effect of the VDGs on CCP2 binding was observed for the 3F3 and 2G9 mAbs (Figure 2B).

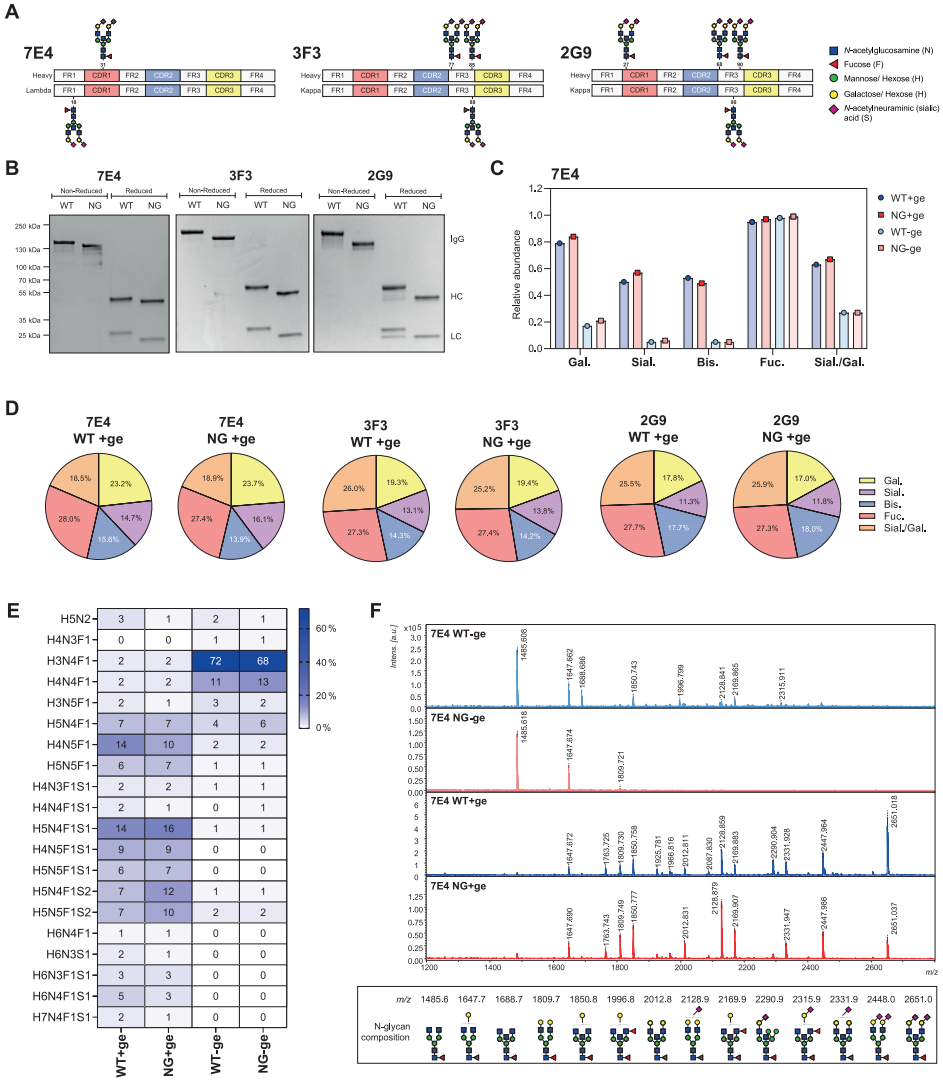

Figure 1. Production of RA patient derived monoclonal ACPA IgG with (wild-type, WT) and without (non-glycosylated, NG) naturally occurring variable domain glycan sites. (**A**) Schematic representation of the 7E4, 3F3 and 2G9 heavy and lambda or kappa light chain variable regions including the respective positions of the naturally occurring N-linked glycan sites. (**B**) 4 to 15% gradient SDS protein gel (BioRad) of purified WT and NG monoclonal ACPA IgG 7E4, 3F3 and 2G9 under non-reduced (IgG) and reduced (HC and LC) conditions. The size-shift caused by the presence of VDGs is visible per mAb-family. The size was determined using the PageRuler™ Plus Prestained Protein Ladder (Thermo Fisher Scientific). (**C**) Relative abundance of Fc galactosylation (Gal.), sialylation (Sial.), bisection (Bis.) and fucosylation (Fuc.) on 7E4 WT and NG +/ge mAb variants determined by LC-MS Fc-glycopeptide analysis. (**D**) Pie chart graphs of WT+ge and NG+ge mAbs 7E4, 3F3 and 2G9. The percentage of galactosylation, sialylation, bisection and fucosylation are shown. (**E**) Fc-peptide glycan compositions of 7E4 WT and NG +/-ge mAb variants. The percentages of the respective glycan traits are shown. (**F**) MALDI-TOF MS analysis of released and stabilized VD and Fc glycans from 7E4 WT and NG +/-ge mAbs. The respective m/z and schematic N-glycan compositions are depicted. Blue square: *N*-acetylglucosamine (GlcNAc), green circle: mannose, yellow circle: galactose, red triangle: fucose, purple diamond: α 2,6-linked *N*-acetylneuraminic acid (sialic acid).

Next, we assessed classical complement pathway activation by addition of exogenous complement (normal human serum, NHS) and subsequent detection of C1q, C4 and C3c deposition on the mAbs bound to the antigen-coated plates (Figure 2A). The findings confirmed the results of previous studies investigating the influence of Fc-glycan compositions on complement activation[30,33], and showed that elevated levels of galactosylation and sialylation, as seen for our glycoengineered (+ge) versus non-glycoengineered (-ge) mAb variants, increased the classical pathway initiation and thus downstream C3c deposition (Figure S3A). Intriguingly, our data showed a substantial reduction in classical pathway activation in the presence of additional glycans attached to the mAb variable domains (WT) (Figure 2C and Figure S3A). We observed a consistently lower degree of C1q, C4 and C3c deposition for all WT mAbs compared to their NG counterparts. No complement activation was detected in the absence of NHS or in the presence of EDTA (Figure 2C). For efficient alternative pathway (AP) activation we used a buffer containing Mg-EGTA, that blocks both the classical and lectin pathway, in the presence of 10% NHS[15]. Under the AP conditions C3c deposition was only marginally reduced when WT antibodies were compared to their NG counterparts, indicating that alternative complement pathway activation is hardly influenced by the presence of VDGs (Figure 2D). No C4 deposition (classical complement pathway component) was observed using the AP-specific buffer (Figure S3D). The effect of VDGs on the classical pathway activation (C1q, C4 and C3c deposition) was observed for all WT compared to their NG mAb variants assessed (Figure 3). The largest difference, particularly for C3c deposition, was noted for the mAb 2G9 (Figure 2C and Figure 3) that expresses in total eight N-linked glycans in the variable domain.

To identify, if VDGs only impact complement activation in the context of ACPA IgG molecules or if this post-translational glycan modification also changes the antibody effector functions for IgG with other specificities, we assessed an anti-TT mAb (D2), which contains one natural LC VDG. Also in this case, we observed a reduced C1q and C3c deposition of the WT mAb compared to its NG counterpart, despite an identical binding to the ELISA plate (Figure S3, B and C).

Next, we investigated whether also polyclonal ACPA IgG with an increased amount of VDGs hinder classical complement activation. To this end, we captured ACPA IgG from two RA patients that showed different VDG quantities. The isolated polyclonal ACPA IgG from patient 2 exhibited, on average, a higher molecular weight likely reflecting a higher degree of VDGs (Figure S4A). This notion was confirmed by LC-MS (Figure S4B) as the obtained glycan profiles revealed a higher degree of the bisected and disialylated glycan traits among the VDGs of ACPA IgG from patient 2 (Figure S4, B and C). In line with our previous observations on the monoclonal level, the polyclonal ACPA IgG with a higher degree of VDGs showed, despite a similar antigen-binding behavior (Figure S4D), a reduced C1q and C3c deposition in the complement activation assay (Figure S4E). We were not able to analyze polyclonal ACPA IgG without VDGs as an increased level of variable domain glycosylation is present in all RA patients. Thus, these results indicate that glycan modifications on the variable domain of both monoclonal and polyclonal antibodies impair C1q binding and the initiation of the classical complement pathway.

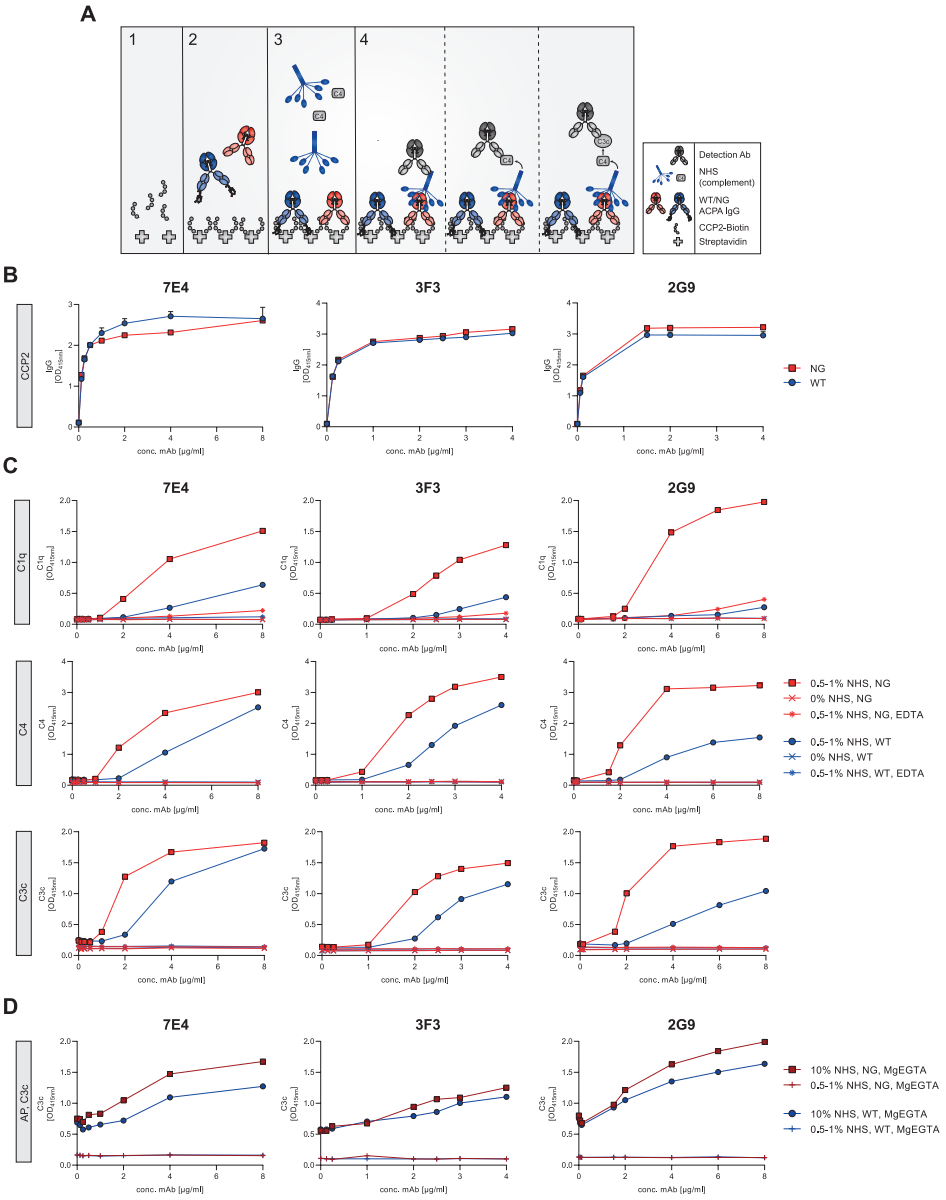

Figure 2. Classical and alternative complement pathway activation of WT vs. NG monoclonal ACPA IgG 7E4 (4× VDGs), 3F3 (6× VDGs) and 2G9 (8× VDGs). (**A**) Schematic representation of the antigen-dependent complement activation assay. Biotinylated CCP2 was added to a streptavidin-coated ELISA plate (1). WT and NG mAbs were added to antigen-coated plates (2). Normal human serum (NHS) containing all complement components was added (3) and complement C1q, C4 and C3c deposition detected (4). (**B**) Detection of WT and NG mAb (7E4, 3F3 and 2G9) binding to CCP2-coated ELISA plates (IgG deposition). (**C**) Classical pathway activation. C1q, C4 and C3c deposition on CCP2 bound WT and NG mAb (7E4, 3F3 and 2G9) in the presence of 0% or 1% NHS in gelatin veronal buffer containing Ca^{2+} and Mg^{2+} (GVB++). (**D**) Alternative pathway (AP) activation. C3c deposition on CCP2 bound WT and NG mAb (7E4, 3F3 and 2G9) in the presence of 1% or 10% NHS in Mg-EGTA buffer.

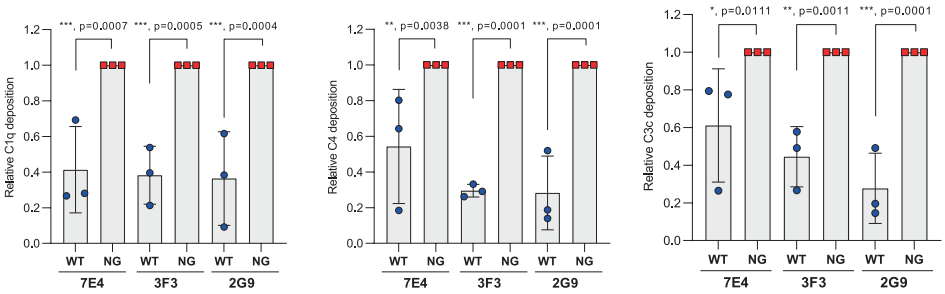

Figure 3. Classical complement pathway activation of WT and NG monoclonal ACPA IgG. Relative C1q, C4 and C3c deposition on CCP2 bound WT mAb compared to its NG counterpart (2 μg/ml). Each experiment was repeated 3 times and each dot represents one independent experiment. Ordinary one-way ANOVA was performed and the respective p-values are depicted: ns $p > 0.05$, *$p \leq 0.05$, **$p \leq 0.01$, ***$p \leq 0.001$ or ****$p \leq 0.0001$.

Impaired C1q binding correlates with the amount of N-linked glycans on the variable domain

We next wished to analyze whether the effect on the initiation of complement activation was dependent on the abundance or location of the N-linked glycans. Therefore, we generated mAb variants of 7E4 and 3F3 with VDGs presented only in the HC (HCWT) or the LC (LCWT), respectively (Figure 4A). As depicted in figure 4B, the apparent molecular weight of the antibodies produced was in line with the number and location of the N-linked glycosylation sites expressed by the respective Ab chains. When assessing these variants in complement activation assays, we observed a clear and significant stepwise decrease in C1q and C3c deposition with an increasing number of VDGs (Figure 4) despite an identical antigen (CCP2)-binding (Figure S5A). The same effect was observed for C4 deposition as assessed using 7E4 (Figure S5, B and C).

In case of 7E4, the glycan expressed by the LC (LCWT) associated with a more potent inhibitory effect compared to the VDG expressed by the HC (HCWT) (Figure 4 and Figure S5). The mAb 3F3 expressing two VDGs in the antibody HC and one in the LC, showed accordingly less complement component deposition when expressed as HCWT variant (Figure 4, C and E). Thus, the data described above indicate that the degree of variable domain glycosylation correlates with its ability to diminish classical complement activation.

To address whether the localization of VDGs in relation to the Fab-arm interacting with its antigen influences the ability of VDGs to hinder classical complement activation, we next generated bispecific antibodies (bsAbs) of the 3F3 clone that is only able to bind with one Fab-arm to its antigenic target. The other arm of the antibody molecule is not "fixed" to the antigen and conceivably flexible and potentially able to interact with the C1q-binding site (Figure 5A). We made use of the structure of the mAb 3F3 co-crystallized with the citrullinated vimentin 59-74 antigen (PDB: 6YXK) and identified T100 located in the HC as the main amino acid involved in citrulline binding. The production of T100V mutants allowed us to generate 3F3 WT and NG

parental mAbs (Figure 5B) unable to bind antigen and, as a consequence, complement (Figure 5C). To generate bsAb molecules with only one citrulline binding arm, we introduced additional mutations in the Fc region allowing a controlled Fab-arm exchange[36]. More specifically, we expressed the 3F3 WT/NG and WT(T100V)/NG(T100V) mutants as parental IgG molecules including two matching point mutations, K409R and F405L respectively, at the C_H3:C_H3 interface. Controlled reduction and reoxidation of the interchain disulfide bonds allowed the mutation-based recombination of H-L pairs resulting in four different 3F3 bsAb (WT+WT(T100V), NG+WT(T100V), WT+NG(T100V) and NG+NG(T100V)) (Figure 5A). The bsAb carrying only one glycosylated Fab-arm (NG+WT(T100V) and WT+NG(T100V) showed a molecular weight between the fully glycosylated and non-glycosylated variants implying a successful Fab-arm exchange of the parental molecules (Figure 5D). Using these antibody variants, we addressed the question whether C1q binding is more restricted when VDGs are located on the Fab-arm directed towards the C1q-docking interface.

Despite similar antigen-binding strengths (Figure 5E), we observed a decreased C1q deposition to the 3F3WT+WT(T100V) bsAb carrying VDGs on either Fab-arm (Figure 5F). The highest C1q binding was observed for the bsAb depicting no VDGs and an intermediate C1q binding for the bsAb molecules with only one variable region glycosylated Fab-arm. No additional inhibitory effect was detected when the glycans were presented on the Fab-arm pointing towards the C1q binding interface or vice versa [(3F3NG+WT(T100V) or 3F3WT+NG(T100V)] (Figure 5F). Consequently, these results indicate that the impairment of complement activation by VDGs is independent of the glycan location in relation to the C1q-binding interface.

Variable domain glycosylation affects the hexamerization potential of IgG

We reasoned that the inhibitory effect of VDGs on complement activation might be caused by a potentially lower ability of Fab-glycosylated IgG to form hexamers (immune complex formation). The latter has been shown essential for the ability of IgG to activate the classical complement pathway[37,38]. Therefore, we next wished to determine the extent to which IgG variable domain glycosylation affects the propensity to form hexamers. For this reason, we generated RGY triple mutants (E345R, E430G and S440Y) of the 3F3 WT and NG mAbs. The combination of these three mutations induces effective IgG hexamerization in solution[38]. We identified the formation of monomeric or oligomeric IgG via size-exclusion chromatography. The data presented in figure 6A reveal predominantly hexameric $(IgG)_6$ species for both the WT and NG RGY mutants at a concentration of 0.5 mg/ml. As expected, the self-assembling RGY mutants showed a reduced hexamer formation at lower concentrations (Figure 6A).

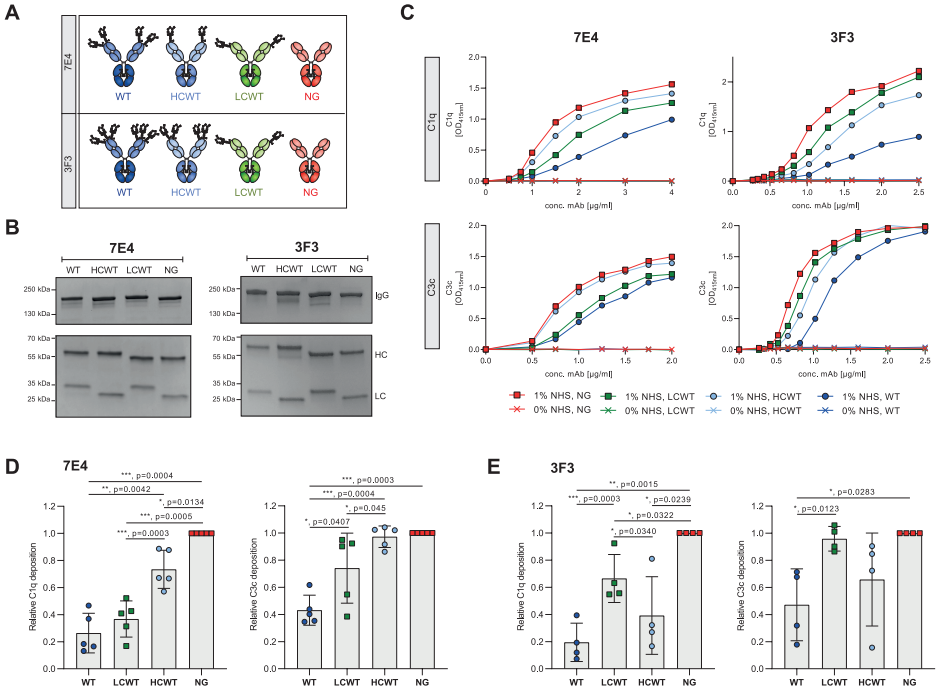

Figure 4. Classical complement pathway activation of monoclonal ACPA IgG 7E4 and 3F3 with a different number of N-linked glycosylation sites in the variable domain of the heavy and light chain. (**A**) Schematic illustration of the generated 7E4 and 3F3 mAbs. (**B**) 4 to 15% gradient SDS protein gel (BioRad) of purified WT HCWT, LCWT and NG monoclonal ACPA IgG 7E4 and 3F3. The size-shift caused by the presence of VDGs is visible per mAb-family. The size was determined using the PageRuler™ Plus Prestained Protein Ladder (Thermo Fisher Scientific). (**C**) Classical complement activation. Detection of C1q and C3c deposition on CCP2 bound WT, HCWT, LCWT and NG 7E4 and 3F3 mAbs in the presence of 0% or 1% NHS in GVB++. (**D**) Relative C1q and C3c deposition on CCP2 bound WT, HCWT, LCWT mAb 7E4 compared to its NG counterpart. Each experiment was repeated 5 times and each dot represents one independent experiment. (**E**) Relative C1q and C3c deposition on CCP2 bound WT, HCWT, LCWT mAb 3F3 compared to its NG counterpart. Each experiment was repeated 4 times and each dot represents one independent experiment. Repeated measure one-way ANOVA was performed including the Geissner-Greenhouse correction. The respective p-values are depicted: ns $p > 0.05$, *$p \leq 0.05$, **$p \leq 0.01$, ***$p \leq 0.001$ or ****$p \leq 0.0001$.

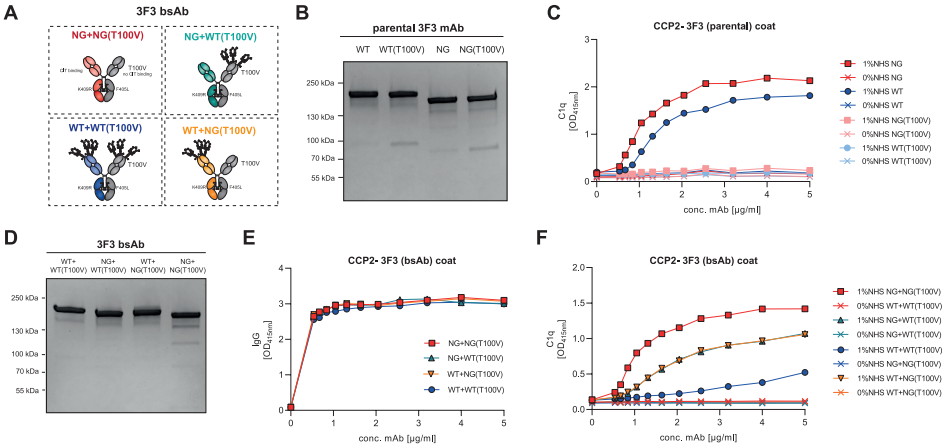

Figure 5. 3F3 bispecific antibodies (bsAb) with only one citrullinated antigen-binding arm (T100V) and varying amounts of VDGs generated via controlled Fab-arm exchange. (**A**) Schematic illustration of the four 3F3 bsAb variants generated including a T100V mutation in one of the Fab-arms to abrogate antigen-specific C1q deposition [NG+NG(T100V), NG+WT(T100V), WT+NG(T100V) and WT+WT(T100V)]. The 3F3 bsAbs harbor a K409R and F405L point-mutation in the C_H3:C_H3 interface to allow controlled Fab-arm exchange[36]. (**B**) 4 to 15% gradient SDS protein gel (BioRad) of the parental 3F3 mAbs under non-reducing (IgG) conditions. The size-shift between the different variants depicts the amount of VDGs present: NG and NG(T100V) < WT and WT(T100V). (**C**) C1q deposition on CCP2 bound parental 3F3 mAbs after adding 0% or 1% NHS in GVB++. (**D**) 4 to 15% gradient SDS protein gel (BioRad) of 3F3 bsAb under non-reducing (IgG) conditions. The size-shift between the different variants depicts the amount of VDGs present: NG+NG(T100V) < NG+WT(T100V) = WT+NG(T100V) < WT+WT(T100V). (**E**) Detection of 3F3 IgG bsAb [WT+WT(T100V), WT+NG(T100V), NG+WT(T100V), NG+NG(T100V] binding to CCP2-coated ELISA plate. (**F**) C1q deposition on CCP2 bound 3F3 bsAbs after adding 0% or 1% NHS in GVB++.

Interestingly, a reduction in hexamer formation was most prominently observed for the WT RGY mutant indicating that under these conditions, the presence of VDGs lowers hexamerization (Figure 6A). Thus, the WT and NG RGY mutants showed different oligomerization efficiencies at the concentrations tested (Figure 6, B and C). The decreased ability of WT RGY mutants to form hexamers was further confirmed by native gel-electrophoresis, showing less prominent intensities at a high molecular weight expected for $(IgG)_6$ molecules as compared to the NG RGY (Figure 6D). The clear size difference between the WT and NG RGY reflects the presence or absence of VDGs (Figure 6, C and D). Despite a similar IgG deposition to the ELISA plate (Figure 6F), we observed, as anticipated, a considerably higher C1q and C3c deposition for the NG RGY mutant compared to the non-mutated monomeric NG variant (Figure 6, E and F). This reflects the increased ability of IgG hexamers to bind C1q as compared to the monomeric molecules when coated to the ELISA plate. When comparing the WT RGY to the NG RGY variant, we detected a significantly decreased C1q and C3c deposition to the variable domain glycosylated variant (Figure 6, E and F). The observed difference in the classical pathway activation is in line with the inhibitory effect of VDGs on the propensity of IgG to form hexamers. An effect of Fc glycans can be excluded as both RGY variants showed a similar Fc glycan composition (Figure S1D).

To further validate the observations described above, we coated the ELISA plate with recombinant C1q and assessed binding of the RGY mutants and the monomeric 3F3 IgG respectively. No binding of the monomeric IgG to C1q was observed (Figure 6G) as IgG is only capable of interacting with C1q in an oligomeric form or when complexed on the ELISA plate. In contrast, the RGY $(IgG)_6$ antibodies showed binding to the recombinant C1q in a dose-dependent manner. Importantly, also in this assay increased interaction with C1q was noted for the NG RGY mutant as compared to the WT RGY mutant (Figure 6G). The presence of NaCl abrogated the binding of both WT and NG RGY mutants to C1q to the same extent, indicating similar affinities of both variants to the C1q globular head domains when oligomerized (Figure S6A). We further confirmed the increased binding of human C1q to the NG RGY mutants compared to their VDG counterparts with western blot analysis (Figure S6D). The data thus show that VDGs decrease the potential of Fc:Fc interactions and thereby affect C1q interactions and complement activity.

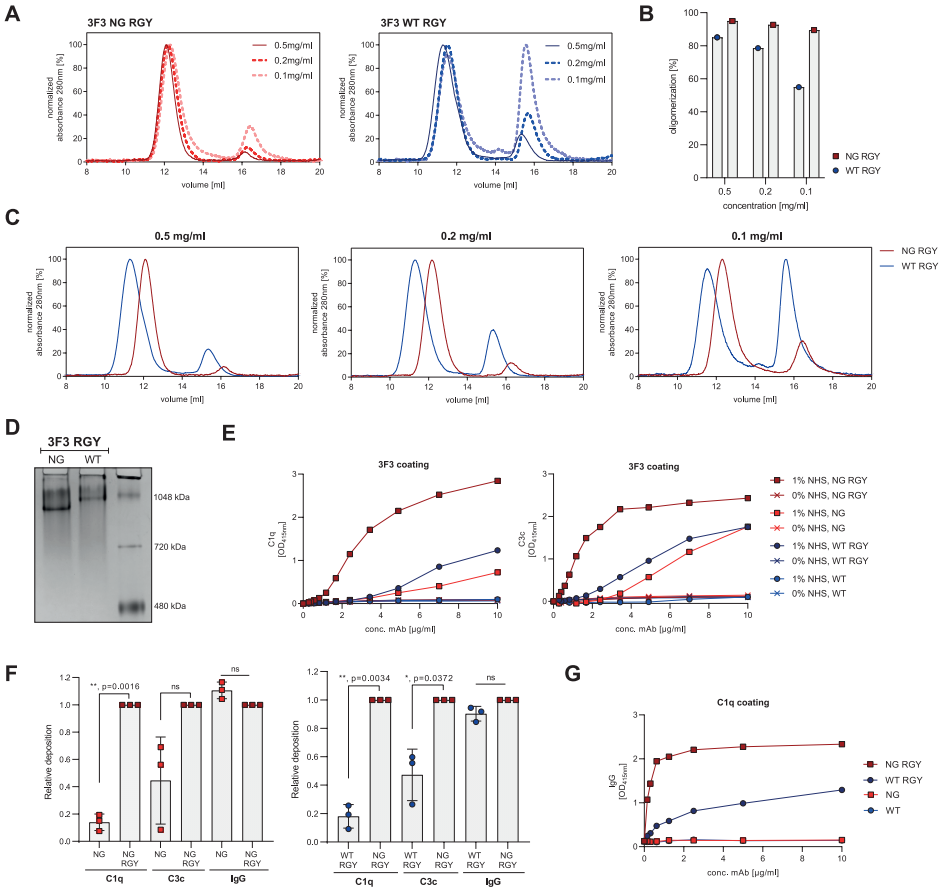

Figure 6. Propensity of 3F3 WT and NG 3F3 mAb IgG RGY mutants to form hexamers and their ability to activate the classical complement pathway. (**A**) Size exclusion chromatograms (SEC) of WT and NG RGY mutants in a concentration dependent manner (0.5 mg/ml, 0.2 mg/ml and 0.1 mg/ml), which elute at a size of oligomeric or monomeric structures. (**B**) Oligomerization efficiency of WT and NG RGY mutants at a concentration of 0.1 mg/ml, 0.2 mg/ml and 0.5 mg/ml. (**C**) Representative SEC chromatogram overlays of WT and NG RGY mutants at the different concentrations analyzed. (**D**) Native 7% TRIS-acetate gel (Novex NuPAGE) of WT and NG RGY mutants depicting a high apparent molecular weight. The size was determined using the NativeMark unstained protein standard (Invitrogen). (**E**) C1q and C3c deposition after mAb WT, NG, WT RGY and NG RGY (0 to 10 µg/ml) coating and in the presence of 0% or 1% NHS in GVB++. (**F**) Relative C1q, C3c and IgG deposition of NG vs. NG RGY and of WT RGY vs. NG RGY. Each experiment was repeated 3 times and each dot represents one independent experiment. Repeated measure one-way ANOVA was performed including the Geissner-Greenhouse correction. The respective p-values are depicted: ns $p > 0.05$, *$p \leq 0.05$, **$p \leq 0.01$, ***$p \leq 0.001$ or ****$p \leq 0.0001$. (**G**) Detection of WT, NG, WT RGY and NG RGY (0 to 10 µg/ml) binding to C1q-coated ELISA plate.

Discussion

The disease-specific autoantibodies from RA patients, ACPA IgG, are hyperglycosylated in the variable domains. Recent studies have shown that the degree of ACPA IgG variable domain glycosylation rises towards RA-onset[17,19] and is predictive for disease development[18], suggesting a functional relevance of this post-translational glycan modification. Intriguingly, VDGs are also profoundly expressed on (auto)antibodies from individuals with AAV, MS, SLE and pSS as well as on inflammation-associated anti-hinge antibodies[26,39-41]. However, in contrast to IgG Fc glycans, the functional significance of IgG VDGs and their contribution to immune effector mechanisms of antibodies are thus far unknown.

In this study, we characterized the impact of hyperglycosylated variable domains on complement initiation and activation. We generated three ACPA IgG and one anti-TT IgG mAb with a different number of naturally occurring VDGs as well as variants with germline-encoded amino acids lacking the N-linked glycan sites. Our results show a notably decreased C1q-binding ability and deposition of classical complement components in the presence of VDGs. We noted greater complement inhibition in the presence of increasing numbers of VDGs, which correlated with a gradual reduction in C1q binding and subsequent C4 and C3c deposition. As no or only a marginal impact of VDGs on the alternative pathway activation was observed, in contrast to a prominent effect on C1q binding, the influence of VDGs to modulate complement activation is likely restricted to the initiation of the classical pathway. Because evolutionary conserved IgG Fc glycans are known to modulate the complement-activating abilities of IgG, we ruled out the possibility that the observed differences were due to variations in Fc glycan compositions. We therefore confirmed that all mAb-pairs (WT and NG) were generated with a similar Fc glycan profile. In line with previous studies, different Fc glycan profiles, as observed for the glycoengineered versus non-glycoengineered mAb variants, showed somewhat elevated complement deposition with increasing levels of Fc galactosylation[30,33].

To provide mechanistic insight into how VDGs regulate the ability of IgG to activate complement, we hypothesized different scenarios. As VDGs affect the (thermo)stability[42] and thus potentially the structure of IgG molecules, we assumed that they may affect the flexibility of the C_H2 domains, the known binding interfaces for C1q. Thereby VDGs may directly alter C1q-binding affinity. However, our data showing a similar abrogated binding of antibodies with or without VDGs in the presence of NaCl, indicate similar avidities of both variants to the C1q globular heads. Another possibility could be that the bulky glycans attached to the variable domain directly interact with C1q. Our results based on bispecific antibody molecules presenting VDGs either in the Fab-arm pointing towards the C1q-binding interface or the Fab-arm interacting with the antigen, argue however against this hypothesis. The position of the VDGs in relation to the C1q-docking site was not relevant

for the dampening effect on C1q binding. A third possibility could be that VDGs alter the spatial orientation of IgG molecules resulting in diminished Fc:Fc interactions and thus hexamerization. This would be in line with previous findings showing that antibody Fab-arms can contribute to immune complex formation and thereby influence C1 activation[38]. Our results also support this scenario, as VDGs decreased the potential of IgG molecules to form hexamers in solution. We observed a decreased tendency of WT RGY variants to form spontaneous hexamers in the absence of their cognate antigen. Accordingly, it can be assumed that glycans attached to variable domain impact on IgG oligomerization, potentially by steric repulsion, which provides a mechanistic explanation for the decreased C1q-binding ability and diminished classical complement activation.

Further studies need to investigate how glycans impact on the oligomerization efficiency of IgG molecules. For example, it still needs to be elucidated, if distinct VDG compositions (differences in sialylation, galactosylation or bisection) impact differently on the oligomerization propensity of IgG. However, this analysis is likely challenging because changes in Fab glycan compositions, due to treatment with specific glycosidases, are always accompanied by changes in the Fc-glycan profile. In addition, it remains to be investigated, whether the location of the N-linked glycan site is important for the observed effects. Based on our results, it is tempting to speculate that glycans attached to the V_L have a more pronounced effect because they may be more flexible and thus sterically more demanding compared to V_H N-linked glycans. However, further studies need to be performed analyzing multiple clones that express V_H or V_L restricted VDGs. Exploring which VDGs have the most pronounced effect on hexamerization and subsequent complement activation, would allow us to specifically design monoclonal antibodies with boostered therapeutic potencies by taming down their Fc domain-mediated effector functions, such as complement-dependent cytotoxicity (CDC).

In conclusion, although it is not possible to conclude from our data, if and how hyperglycosylated autoantibodies from RA patients contribute to disease pathogenesis or if they might have a protective effect, our results clearly show that a post-translational glycan modification on top of the IgG variable domain can be exploited to "switch off" the antibody-dependent classical complement pathway.

Materials and Methods

Blood samples from patients diagnosed with RA – Peripheral blood samples from ACPA-positive ($ACPA^+$, > 340 U/ml) patients with RA visiting the outpatient clinic of the Rheumatology Department at the Leiden University Medical Center (LUMC) were included in this study. All patients fulfilled the EULAR/ACR 2010-criteria for classification of RA[43]. None of the patients

were previously treated with B-cell depletion therapies. Blood samples were obtained on written informed consent prior to inclusion and with approval from the local ethics committee of the LUMC, The Netherlands. Patient characteristics were previously described[44].

Recombinant mAb production, generation of RGY mutants and bsAb molecules – Monoclonal antibodies (mAbs) were generated based on full-length BCR sequences from ACPA-positive patients with RA or healthy donors. Labelled CCP2- and CArgP2-streptavidin tetramers or tetanus toxoid (TT) (Statens Serum Institute) were used to single cell isolate ACPA or anti-TT-expressing B cells as previously described[45]. RNA isolation, cDNA synthesis, ARTISAN PCR and BCR sequencing were performed as described earlier[27,46]. The 7E4 sequence was provided by Dr. Rispens, Sanquin, The Netherlands[47]. To generate mAbs without the naturally occurring variable domain glycans, N-linked glycan motifs (N-X-S/T, X ≠ P) in the Fab-domains were specifically mutated back to the germline amino acid sequence (based on IMGT) at the respective position (Table S1). Wild-type (WT), including N-linked glycan sites, and non-glycosylated (NG), including only the conserved Fc N-linked glycan sites, BCR sequences were codon-optimized and the HC/LC variable genes together with 5'-BamHI and 3'-XhoI restriction sites, the Kozak sequence, and the IGHV1-18*01 leader sequence ordered from GeneArt (Life Technologies). The constructs were ligated into the pcDNA3.1 (+) expression vector (Invitrogen) carrying the IGHG1 or the IGLC3/IGKC constant regions (UniProt) respectively flanking 3'-XhoI site. The recombinant monoclonal antibodies were produced in Freestyle™ 293-F cells (Gibco) as previously stated[44]. Glycoengineering (ge) was performed by adding D-galactose substrate (Sigma, G0750-5G) and by a co-transfection with 1% β-1,4-*N*-acetylglucosaminyltransferase III (GnTIII), 2.5% α2,6-sialyltransferase 1 (ST6galT) and 1% β-1,4-galactosyltransferase 1 (B4GalT1). The supernatants were harvested 5 to 6 days post-transfection. IgG1 antibodies were purified using a 1 ml HiTrap® Protein G HP affinity column (GE Healthcare) followed by a direct buffer exchange (53 ml HiPrep™ 26/10 Desalting column, GE Healthcare). In total three ACPA (7E4, 3F3 and 2G9) and one anti-TT (D2) monoclonal were generated as IgG1. Additionally, we produced the 7E4 and 3F3 mAbs with only the HC (HCWT) or the LC (LCWT) N-linked glycans, respectively. For RGY mutants, the 3F3 WT and NG HC were generated including three point-mutations (E345R, E430G and S440Y) in the IGHG1*01 constant domain[37]. The mutated HC sequences were ordered from GeneArt (Life Technologies) and cloned as described above. 3F3 RGY mutants were produced in Freestyle™ 293-F cells (Gibco) with glycoengineering as mentioned above.

To produce 3F3 bispecific antibodies (bsAbs) that bind only with one Fab-arm to citrullinated antigens, we made use of the 3F3 crystal structure (PDB: 6YXK) and introduced the T100V point-mutation into the HC CDR3. Next, two matching point-mutations, K409R and F405L, were introduced into the C_H3 interface of 3F3WT/NG or 3F3WT(T100V)/NG(T100V), respectively. All point-mutations were introduced using the Q5 Site-Directed Mutagenesis Kit (NEB,E0554S). After the production of the parental 3F3 WT(K409R), NG(K409R), WT(T100V, F405L) and NG(T100V,

F405L) mAbs in Freestyle™ 293-F cells (Gibco) as described above, the bsAb molecules were generated with the controlled Fab-arm exchange method as previously described[36]. In brief, 50 μg of the parental 3F3 mAb pairs were mixed in equimolar amounts and incubated with 750 mM cysteamide hydrochloride (Sigma Aldrich) for 5 hours at 31 °C for reduction. Reoxidation and buffer exchange was performed using ultra centrifugal filters (50,000 MWCO, Merck Millipore) and PBS. This method allows a mutation-based recombination of HC-LC pairs resulting in four 3F3 bsAb molecules [WT+WT(T100V), NG+WT(T100V), WT+NG(T100V) and NG+NG(T100V)].

Integrity and size characterization of mAbs – The human mAb integrity and the expression of the VDGs was analyzed via size-exclusion chromatography (SEC), SDS gel electrophoresis and native gel electrophoresis**.** SEC was performed using a Superose6Increase, 10/300 GL column (GE Healthcare). The recombinant proteins were monitored by UV absorption at 280 nm. For sodium dodecyl sulfate (SDS) polyacrylamide gel electrophoresis (PAGE), 1.5 μg of the mAbs were diluted in 4× Laemmli buffer (Bio Rad) with (reduced) or without (non-reduced) 2% β-mercaptoethanol (Sigma Aldrich) and incubated for 5 min at 95 °C. Samples and PageRuler™ Plus Prestained Protein Ladder (Thermo Fisher Scientific) were loaded on 4 to 15% SDS-polyacrylamide gels (Bio Rad). For native gel electrophoresis, 1 to 4 μg of the RGY mutants were diluted in 2× TRIS-glycine native sample buffer (Novex) and applied to a 7% TRIS-acetate gel (Novex NuPAGE) together with the NativeMark Unstained Protein Standard (Invitrogen). For protein detection gels were stained with Coomassie Brilliant Blue G-250 Dye (Thermo Fisher Scientific).

Fc-glycopeptide and variable domain glycosylation mass spectrometry (MS) analysis – Matrix Assisted Laser Desorption Ionization Time of Flight (MALDI-TOF) MS analysis of released N-glycans was performed as previously described[48]. In brief, the IgG samples (10 μg) were reduced in 2% SDS and incubated with 0.5 U N-glycosidase F, PNGase F, (Roche Diagnostics, Germany), in 1:1 5xPBS/ 4% NP-40, overnight at 37 °C. The total released glycans were stabilized with ethylation reagent (0.5 M EDC hydrochloride and 0.5 M 1-hydroxybenzotriazole hydrate) for 1 hour at 37 °C. Glycans were purified in 85% acetonitrile (ACN) (Biosolve, Valkenswaard, The Netherlands) with 15 μl cotton hydrophilic interaction liquid chromatography (HILIC) tips using 85% ACN and 85% ACN+1% TFA for washing. Released and purified N-glycans were eluted from the HILIC tips using MQ and 1 μl spotted on a MALDI target (MTP AnchorChip 800/384 TF; Bruker Daltonics) together with 1 μl 5 mg/ml super-DHB in 50% ACN and 1 mM NaOH. Spots were dried on room temperature (RT) and analyzed on an UltrafleXtreme (Bruker Daltonics) operated under flexControl 3.3 (Build 108; Bruker Daltonics). A mass spectrum from m/z 1000 to 3000 was recorded, combining 10000 shots in a random walk pattern at 1000 Hz. The instrument was calibrated with a peptide calibration standard (Bruker Daltonics). MS data were analyzed using flexControl 3.3 and glycan peaks above S/N of nine were included into the analysis.

Liquid chromatography-mass spectrometry (LC-MS) Fc-glycopeptide analysis was performed as previously described[49]. Briefly, denatured mAbs were trypsinized using 200 ng sequencing grade modified trypsin (Promega) in 50 mM ammonium bicarbonate overnight at 37 °C. For total N-glycan LC-MS analysis, glycans were released using 2 U PNGase F as described above, labeled with 2-aminobenzoic acid (2-AA, Sigma Aldrich) and 2-picoline borane (2-PB, Sigma Aldrich) and purified using 15 ul cotton HILIC tips as described earlier. Trypsinized samples or released and purified glycans were separated and analyzed on an Ultimate 3000 UHPLC system (Dionex/ Thermo Fisher Scientific, Breda, The Netherlands) coupled to a MaXis Impact HD quadrupole-TOF mass spectrometer (MaXis HD, Bruker Daltonics, Bremen, Germany) equipped with a CaptiveSpray NanoBooster source (Bruker Daltonics, Bremen, Germany) as previously described[49-51]. Mass spectra were acquired within a mass range of m/z 550 to 1800. LC-MS data were first examined manually using DataAnalysis (Bruker Daltonics). Data processing, including peak integration, was performed using LaCyTools v1.1.0. Glycans with a S/N above nine, a mass accuracy of +/-20 and an isotopic peak quality (IPQ) of 0.2 were included into the analysis[52].

Complement activation assays – To analyze the complement activating potential of mAbs with different quantities of VDGs, enzyme-linked immunosorbent assays (ELISA) were performed in a similar way than previously described[15]. In short, mAbs were coated directly to Nunc Maxisorp plates (Thermo Fisher Scientific) in coating buffer [100 mM Na2CO3/NaHCO3 (pH 9.6)] overnight at 4 °C. Or mAbs were diluted in PBS/ 0.05%Tween/ 1% BSA (PBT) and added to streptavidin plates (Microcoat, #65001) pre-coated with biotinylated CCP2 (1 μg/ml) overnight at 4 °C[44]. The mAb concentrations used are mentioned in the respective figure legends. To obtain a similar coating, the CCP2 concentrations were adjusted for the 7E4 WT (1.9 μg/ml) and NG (0.95 μg/ml) mAb variants. Comparable deposition of WT and NG mAbs to the ELISA plate was verified using a HRP-conjugated rabbit-anti-human IgG secondary detection antibody (DAKO, P0214, 1:5000).

For complement activation, 0%, 0.5%, 1% or 10% complement-active normal human serum (NHS) diluted either in GVB++ (veronal buffered saline [VBS] containing 0.5 mM MgCl2, 2 mM CaCl2, 0.05% Tween 20, and 0.1% gelatin [pH7.5]) or Mg-EGTA (VBS containing 10 mM EGTA, 5 mM MgCl2, 0.05% Tween 20, and 0.1% gelatin [pH 7.5]) buffer was added for 1 hour at 37 °C. Complement deposition on the mAbs was determined by adding rabbit anti-C1q (DAKO, A0136, 1:1000), goat anti-C4 (QUIDEL, A305, 1:1000) or rabbit anti-C3c (DAKO, A0062, 1:1000) secondary antibodies in PBT for 1 hour at 37 °C. Binding was detected using matched and HRP-labelled goat anti-rabbit (DAKO, P0448, 1:3000) or rabbit anti-goat (DAKO, P0449, 1:3000) detection antibodies diluted in PBT for 1 hour at 37 °C. The plates were developed using the substrate ABTS, and absorbance was read at 415 nm. A schematic overview of this assay is shown in figure 2A. To identify direct interactions with C1q, 10 μg/ml of the recombinant C1q protein was directly coated to Nunc Maxisorp plates (Thermo Fisher Scientific) in coating buffer

for 1 hour at 37 °C. After blocking with PBS/ 1% BSA for 1 hour at 37 °C, mAbs were added in PBT and incubated for 1 hour at 37 °C. Binding of the IgG mAbs to C1q was detected using HRP-labelled F(ab')^2 Fragment rabbit anti-human IgG (Jackson ImmunoResearch, #309-036-003) diluted 1:5000 in PBT and incubated for 1 hour at 37 °C. The plates were developed using the substrate ABTS, and absorbance was read at 415 nm.

Western blot analysis – C1q binding to the 3F3 WT and NG RGY mutants was analyzed via western blot analyses. Therefore, 1 to 4 μg of the respective RGY mutants was diluted in 2× TRIS-glycine native sample buffer (Novex) and applied to a 7% TRIS-acetate gel (Novex NuPAGE). The native gel was incubated for 1 hour in a buffer containing 0.05% SDS, 0.0125M Tris and 0.1 M glycine to achieve a negative protein charge and subsequently immunoblotted on a Nitrocellulose membrane (Bio Rad). The blot was incubated in PTE (3% skim milk powder/ PBS/0.05% tween) for 1 hour at RT. Following washing with PBS/0.05% tween (PT), the blot was incubated at 4 °C overnight with 8 μg human native C1q (CompTech) diluted in 5 ml PTE. After washing with PT, the blot was incubated for 1 hour at RT with 5 ml PTE containing 1:1000 rabbit anti-human C1q (#A0136, DAKO). Binding was detected using an HRP-labelled goat anti-rabbit (DAKO, P0448, 1:1000) detection antibody diluted in PT for 2 hours at 37 °C. The blot was washed and bound antibodies visualized using enhanced chemiluminescence (GE Healthcare, RPN2109). The readout was performed on a Bio Rad Chemidoc Touch Imaging system.

Statistical analysis – Repeated measure (RM) one-way ANOVA including the Geissner-Greenhouse correction, ordinary (no pairing) one-way ANOVA or paired t-tests were performed using the GraphPad Prism software (GraphPad Prism 8.0.1 software). P values less than 0.05 were considered significant: ns $p > 0.05$, *$p \leq 0.05$, **$p \leq 0.01$, ***$p \leq 0.001$ or ****$p \leq 0.0001$.

Acknowledgments

We thank J.-W. Drijfhout (LUMC, Leiden, The Netherlands) for providing the citrullinated peptides.

Funding

This work was supported by ReumaNederland 17-1-402 (to R.E.M.T.), the IMI-funded project RTCure 777357 (to T.W.J.H.), ZonMw TOP 91214031 (to R.E.M.T.), Target-to-B LSHM18055-SGF (to R.E.M.T.), NWO-ZonMW clinical fellowship 90714509 (to H.U.S.), NWO-ZonMW VENI grant 91617107 (to H.U.S.), ZonMW Enabling Technology Hotels grant 435002030 (to H.U.S.) and the Dutch Arthritis Foundation 15-2-402 and 18-1-205 (to H.U.S.).

Author contributions

All authors were involved in drafting the article or revising it critically for important intellectual content, and all authors approved the final version to be published. Conceptualization: T.K. and R.E.M.T. Methodology: T.K., S.v.d.B., H.J.v.D., A.S.B., J.C.K., E.M.S., C.K. Investigation: T.K., S.v.d.B., H.J.v.D., A.S.B., E.M.S. Visualization: T.K. Supervision: L.A.T. and R.E.M.T. Writing—original draft: T.K. and R.E.M.T. Writing—review and editing: T.K., S.v.d.B., H.J.v.D., A.S.B., J.C.K., E.M.S., C.K., M.W., T.W.J.H., H.U.S., L.A.T. and R.E.M.T.

Conflict of interest

H.U.S., T.W.J.H., and R.E.M.T. are mentioned as inventors on a patent on ACPA IgG V-domain glycosylation. The other authors declare that they have no competing interests.

Data and materials availability

We confirm that the data supporting the findings of this study are available within the article and/or the Supplementary Materials. The 7E4 sequence and antibodies can be provided by T.R. (Sanquin Research, The Netherlands) under the protection of a completed material transfer agreement.

References

1 Walport, M. J., Complement. Second of two parts. *N Engl J Med* 2001. 344: 1140-1144.

2 Walport, M. J., Complement. First of two parts. *N Engl J Med* 2001. 344: 1058-1066.

3 Trouw, L. A., Blom, A. M. and Gasque, P., Role of complement and complement regulators in the removal of apoptotic cells. *Mol Immunol* 2008. 45: 1199-1207.

4 Sjoberg, A. P., Trouw, L. A. and Blom, A. M., Complement activation and inhibition: a delicate balance. *Trends Immunol* 2009. 30: 83-90.

5 Dhillon, S., Eculizumab: A Review in Generalized Myasthenia Gravis. *Drugs* 2018. 78: 367-376.

6 Jayne, D. R. W., Bruchfeld, A. N., Harper, L., Schaier, M., Venning, M. C., Hamilton, P., et al., Randomized Trial of C5a Receptor Inhibitor Avacopan in ANCA-Associated Vasculitis. *J Am Soc Nephrol* 2017. 28: 2756-2767.

7 Wouters, D., Voskuyl, A. E., Molenaar, E. T., Dijkmans, B. A. and Hack, C. E., Evaluation of classical complement pathway activation in rheumatoid arthritis: measurement of C1q-C4 complexes as novel activation products. *Arthritis Rheum* 2006. 54: 1143-1150.

8 Brodeur, J. P., Ruddy, S., Schwartz, L. B. and Moxley, G., Synovial fluid levels of complement SC5b-9 and fragment Bb are elevated in patients with rheumatoid arthritis. *Arthritis Rheum* 1991. 34: 1531-1537.

9 Swaak, A. J., Van Rooyen, A., Planten, O., Han, H., Hattink, O. and Hack, E., An analysis of the levels of complement components in the synovial fluid in rheumatic diseases. *Clin Rheumatol* 1987. 6: 350-357.

10 Konttinen, Y. T., Ceponis, A., Meri, S., Vuorikoski, A., Kortekangas, P., Sorsa, T., et al., Complement in acute and chronic arthritides: assessment of C3c, C9, and protectin (CD59) in synovial membrane. *Ann Rheum Dis* 1996. 55: 888-894.

11 Nielen, M. M., van Schaardenburg, D., Reesink, H. W., van de Stadt, R. J., van der Horst-Bruinsma, I. E., de Koning, M. H., et al., Specific autoantibodies precede the symptoms of rheumatoid arthritis: a study of serial measurements in blood donors. *Arthritis Rheum* 2004. 50: 380-386.

12 van Boekel, M. A., Vossenaar, E. R., van den Hoogen, F. H. and van Venrooij, W. J., Autoantibody systems in rheumatoid arthritis: specificity, sensitivity and diagnostic value. *Arthritis Res* 2002. 4: 87-93.

13 van Gaalen, F. A., Linn-Rasker, S. P., van Venrooij, W. J., de Jong, B. A., Breedveld, F. C., Verweij, C. L., et al., Autoantibodies to cyclic citrullinated peptides predict progression to rheumatoid arthritis in patients with undifferentiated arthritis: a prospective cohort study. *Arthritis Rheum* 2004. 50: 709-715.

14 Kuhn, K. A., Kulik, L., Tomooka, B., Braschler, K. J., Arend, W. P., Robinson, W. H., et al., Antibodies against citrullinated proteins enhance tissue injury in experimental autoimmune arthritis. *J Clin Invest* 2006. 116: 961-973.

15 Trouw, L. A., Haisma, E. M., Levarht, E. W., van der Woude, D., Ioan-Facsinay, A., Daha, M. R., et al., Anti-cyclic citrullinated peptide antibodies from rheumatoid arthritis patients activate complement via both the classical and alternative pathways. *Arthritis Rheum* 2009. 60: 1923-1931.

16 Hafkenscheid, L., Bondt, A., Scherer, H. U., Huizinga, T. W., Wuhrer, M., Toes, R. E., et al., Structural Analysis of Variable Domain Glycosylation of Anti-Citrullinated Protein Antibodies in Rheumatoid Arthritis Reveals the Presence of Highly Sialylated Glycans. *Mol Cell Proteomics* 2017. 16: 278-287.

17 Kissel, T., van Schie, K. A., Hafkenscheid, L., Lundquist, A., Kokkonen, H., Wuhrer, M., et al., On the presence of HLA-SE alleles and ACPA-IgG variable domain glycosylation in the phase preceding the development of rheumatoid arthritis. *Ann Rheum Dis* 2019. 78: 1616-1620.

18 Hafkenscheid, L., de Moel, E., Smolik, I., Tanner, S., Meng, X., Jansen, B. C., et al., N-Linked Glycans in the Variable Domain of IgG Anti-Citrullinated Protein Antibodies Predict the Development of Rheumatoid Arthritis. *Arthritis Rheumatol* 2019. 71: 1626-1633.

19 Kissel, T., Hafkenscheid, L., Wesemael, T. J., Tamai, M., Kawashiri, S. Y., Kawakami, A., et al., ACPA-IgG variable domain glycosylation increases before the onset of rheumatoid arthritis and stabilizes thereafter; a cross-sectional study encompassing 1500 samples. *Arthritis Rheumatol* 2022.

20 Vergroesen, R. D., Slot, L. M., Hafkenscheid, L., Koning, M. T., van der Voort, E. I. H., Grooff, C. A., et al., B-cell receptor sequencing of anti-citrullinated protein antibody (ACPA) IgG-expressing B cells indicates a selective advantage for the introduction of N-glycosylation sites during somatic hypermutation. *Ann Rheum Dis* 2018. 77: 956-958.

21 Vergroesen, R. D., Slot, L. M., van Schaik, B. D. C., Koning, M. T., Rispens, T., van Kampen, A. H. C., et al., N-Glycosylation Site Analysis of Citrullinated Antigen-Specific B-Cell Receptors Indicates Alternative Selection Pathways During Autoreactive B-Cell Development. *Front Immunol* 2019. 10: 2092.

22 Kissel, T., Ge, C., Hafkenscheid, L., Kwekkeboom, J. C., Slot, L. M., Cavallari, M., et al., Surface Ig variable domain glycosylation affects autoantigen binding and acts as threshold for human autoreactive B cell activation. *Sci Adv* 2022. 8: eabm1759.

23 Kasermann, F., Boerema, D. J., Ruegsegger, M., Hofmann, A., Wymann, S., Zuercher, A. W., et al., Analysis and functional consequences of increased Fab-sialylation of intravenous immunoglobulin (IVIG) after lectin fractionation. *PLoS One* 2012. 7: e37243.

24 Xu, P. C., Gou, S. J., Yang, X. W., Cui, Z., Jia, X. Y., Chen, M., et al., Influence of variable domain glycosylation on anti-neutrophil cytoplasmic autoantibodies and anti-glomerular basement membrane autoantibodies. *BMC Immunol* 2012. 13: 10.

25 Hamza, N., Hershberg, U., Kallenberg, C. G., Vissink, A., Spijkervet, F. K., Bootsma, H., et al., Ig gene analysis reveals altered selective pressures on Ig-producing cells in parotid glands of primary Sjogren's syndrome patients. *J Immunol* 2015. 194: 514-521.

26 Visser, A., Hamza, N., Kroese, F. G. M. and Bos, N. A., Acquiring new N-glycosylation sites in variable regions of immunoglobulin genes by somatic hypermutation is a common feature of autoimmune diseases. *Ann Rheum Dis* 2018. 77: e69.

27 Huijbers, M. G., Vergoossen, D. L., Fillie-Grijpma, Y. E., van Es, I. E., Koning, M. T., Slot, L. M., et al., MuSK myasthenia gravis monoclonal antibodies: Valency dictates pathogenicity. *Neurol Neuroimmunol Neuroinflamm* 2019. 6: e547.

28 Mandel-Brehm, C., Fichtner, M. L., Jiang, R., Winton, V. J., Vazquez, S. E., Pham, M. C., et al., Elevated N-Linked Glycosylation of IgG V Regions in Myasthenia Gravis Disease Subtypes. *J Immunol* 2021. 207: 2005-2014.

29 van de Bovenkamp, F. S., Derksen, N. I. L., Ooijevaar-de Heer, P., van Schie, K. A., Kruithof, S., Berkowska, M. A., et al., Adaptive antibody diversification through N-linked glycosylation of the immunoglobulin variable region. *Proc Natl Acad Sci U S A* 2018. 115: 1901-1906.

30 Dekkers, G., Treffers, L., Plomp, R., Bentlage, A. E. H., de Boer, M., Koeleman, C. A. M., et al., Decoding the Human Immunoglobulin G-Glycan Repertoire Reveals a Spectrum of Fc-Receptor- and Complement-Mediated-Effector Activities. *Front Immunol* 2017. 8: 877.

31 Lund, J., Takahashi, N., Pound, J. D., Goodall, M. and Jefferis, R., Multiple interactions of IgG with its core oligosaccharide can modulate recognition by complement and human Fc gamma receptor I and influence the synthesis of its oligosaccharide chains. *J Immunol* 1996. 157: 4963-4969.

32 Tao, M. H. and Morrison, S. L., Studies of aglycosylated chimeric mouse-human IgG. Role of carbohydrate in the structure and effector functions mediated by the human IgG constant region. *J Immunol* 1989. 143: 2595-2601.

33 Peschke, B., Keller, C. W., Weber, P., Quast, I. and Lunemann, J. D., Fc-Galactosylation of Human Immunoglobulin Gamma Isotypes Improves C1q Binding and Enhances Complement-Dependent Cytotoxicity. *Front Immunol* 2017. 8: 646.

34 Quast, I., Keller, C. W., Maurer, M. A., Giddens, J. P., Tackenberg, B., Wang, L. X., et al., Sialylation of IgG Fc domain impairs complement-dependent cytotoxicity. *J Clin Invest* 2015. 125: 4160-4170.

35 van Osch, T. L. J., Nouta, J., Derksen, N. I. L., van Mierlo, G., van der Schoot, C. E., Wuhrer, M., et al., Fc Galactosylation Promotes Hexamerization of Human IgG1, Leading to Enhanced Classical Complement Activation. *J Immunol* 2021. 207: 1545-1554.

36 Labrijn, A. F., Meesters, J. I., Priem, P., de Jong, R. N., van den Bremer, E. T., van Kampen, M. D., et al., Controlled Fab-arm exchange for the generation of stable bispecific IgG1. *Nat Protoc* 2014. 9: 2450-2463.

37 Diebolder, C. A., Beurskens, F. J., de Jong, R. N., Koning, R. I., Strumane, K., Lindorfer, M. A., et al., Complement is activated by IgG hexamers assembled at the cell surface. *Science* 2014. 343: 1260-1263.

38 Wang, G., de Jong, R. N., van den Bremer, E. T., Beurskens, F. J., Labrijn, A. F., Ugurlar, D., et al., Molecular Basis of Assembly and Activation of Complement Component C1 in Complex with Immunoglobulin G1 and Antigen. *Mol Cell* 2016. 63: 135-145.

39 Vletter, E. M., Koning, M. T., Scherer, H. U., Veelken, H. and Toes, R. E. M., A Comparison of Immunoglobulin Variable Region N-Linked Glycosylation in Healthy Donors, Autoimmune Disease and Lymphoma. *Front Immunol* 2020. 11: 241.

40 Biermann, M. H., Griffante, G., Podolska, M. J., Boeltz, S., Sturmer, J., Munoz, L. E., et al., Sweet but dangerous - the role of immunoglobulin G glycosylation in autoimmunity and inflammation. *Lupus* 2016. 25: 934-942.

41 Kempers, A. C., Hafkenscheid, L., Dorjee, A. L., Moutousidou, E., van de Bovenkamp, F. S., Rispens, T., et al., The extensive glycosylation of the ACPA variable domain observed for ACPA-IgG is absent from ACPA-IgM. *Ann Rheum Dis* 2018. 77: 1087-1088.

42 van de Bovenkamp, F. S., Derksen, N. I. L., van Breemen, M. J., de Taeye, S. W., Ooijevaar-de Heer, P., Sanders, R. W., et al., Variable Domain N-Linked Glycans Acquired During Antigen-Specific Immune Responses Can Contribute to Immunoglobulin G Antibody Stability. *Front Immunol* 2018. 9: 740.

43 Aletaha, D., Neogi, T., Silman, A. J., Funovits, J., Felson, D. T., Bingham, C. O., 3rd, et al., 2010 rheumatoid arthritis classification criteria: an American College of Rheumatology/European League Against Rheumatism collaborative initiative. *Ann Rheum Dis* 2010. 69: 1580-1588.

44 Kissel, T., Reijm, S., Slot, L. M., Cavallari, M., Wortel, C. M., Vergroesen, R. D., et al., Antibodies and B cells recognising citrullinated proteins display a broad cross-reactivity towards other post-translational modifications. *Ann Rheum Dis* 2020. 79: 472-480.

45 Kerkman, P. F., Fabre, E., van der Voort, E. I., Zaldumbide, A., Rombouts, Y., Rispens, T., et al., Identification and characterisation of citrullinated antigen-specific B cells in peripheral blood of patients with rheumatoid arthritis. *Ann Rheum Dis* 2016. 75: 1170-1176.

46 Koning, M. T., Kielbasa, S. M., Boersma, V., Buermans, H. P. J., van der Zeeuw, S. A. J., van Bergen, C. A. M., et al., ARTISAN PCR: rapid identification of full-length immunoglobulin rearrangements without primer binding bias. *Br J Haematol* 2017. 178: 983-986.

47 van de Stadt, L. A., van Schouwenburg, P. A., Bryde, S., Kruithof, S., van Schaardenburg, D., Hamann, D., et al., Monoclonal anti-citrullinated protein antibodies selected on citrullinated fibrinogen have distinct targets with different cross-reactivity patterns. *Rheumatology (Oxford)* 2013. 52: 631-635.

48 Reiding, K. R., Lonardi, E., Hipgrave Ederveen, A. L. and Wuhrer, M., Ethyl Esterification for MALDI-MS Analysis of Protein Glycosylation. *Methods Mol Biol* 2016. 1394: 151-162.

49 Rombouts, Y., Ewing, E., van de Stadt, L. A., Selman, M. H., Trouw, L. A., Deelder, A. M., et al., Anti-citrullinated protein antibodies acquire a pro-inflammatory Fc glycosylation phenotype prior to the onset of rheumatoid arthritis. *Ann Rheum Dis* 2015. 74: 234-241.

50 Plomp, R., de Haan, N., Bondt, A., Murli, J., Dotz, V. and Wuhrer, M., Comparative Glycomics of Immunoglobulin A and G From Saliva and Plasma Reveals Biomarker Potential. *Front Immunol* 2018. 9: 2436.

51 Selman, M. H., Derks, R. J., Bondt, A., Palmblad, M., Schoenmaker, B., Koeleman, C. A., et al., Fc specific IgG glycosylation profiling by robust nano-reverse phase HPLC-MS using a sheath-flow ESI sprayer interface. *J Proteomics* 2012. 75: 1318-1329.

52 Jansen, B. C., Falck, D., de Haan, N., Hipgrave Ederveen, A. L., Razdorov, G., Lauc, G., et al., LaCyTools: A Targeted Liquid Chromatography-Mass Spectrometry Data Processing Package for Relative Quantitation of Glycopeptides. *J Proteome Res* 2016. 15: 2198-2210.

Supplemental Tables

Table S1. ACPA IgG BCR variable region sequence details. ACPA IgG BCR sequences isolated from single B cells of 3 RA patients and anti-TT IgG BCR sequence isolated from a healthy donor. Immunoglobulin (IG) heavy and kappa (K) or lambda (L) light chain CDR3 amino-acid sequences are depicted. The N-linked glycan motifs presented in the variable heavy (V_H) or light (V_L) chain are visualized together with their respective location. The germline motifs are depicted based on the IMGT database.

IgG	Patient	IGH-CDR3	IGK/L-CDR3
7E4 (ACPA)	4	CVRIRGGSSNW	CAAWNGRLSAFVF
2G9 (ACPA)	2	CVRWGEDRTEGLW	CMQRLRFPLTF
3F3 (ACPA)	1	CARGTYLPVDESAAFDVW	CQQYYEAPYTF
D2 (anti-TT)	7	CARRGGKDNVWGDW	CQQYNDWPVTF

* Amino-acid sequence and location.

† Determined by IMGT/ V-QUEST.

N-linked glycan motifs V_H*	N-linked glycan motifs V_L*	Germline motifs V_H†	Germline motifs V_L†
NES (CDR1)	NVT (FR1)	SES (CDR1)	KVT (FR1)
NGS (CDR1), NTS (FR3) and NMT (FR3)	NIS (FR3)	GGS (CDR1), NPS (FR3) and KLS (FR3)	KIS (FR3)
NMT (FR3) and NTS (FR3)	NLT (FR3)	TMT (FR3) and STA (FR3)	TLT (FR3)
NFT (CDR1)	x	SFT (CDR1)	x

Supplemental Figures

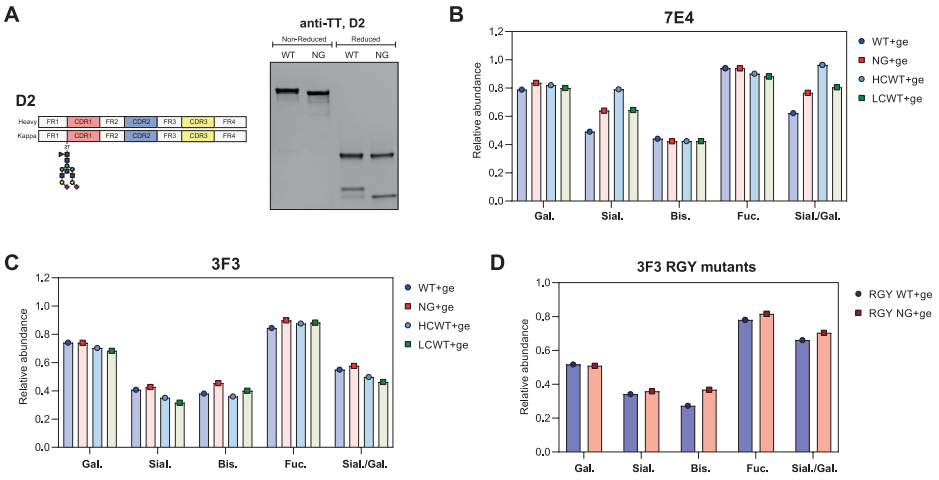

Figure S1. Production data of monoclonal ACPA and anti-TT IgG with (wild-type, WT) and without (non-glycosylated, NG) naturally occurring VDGs. (**A**) Schematic depiction of the D2 (anti-TT) heavy and kappa light chain variable regions including the position of the naturally occurring N-linked glycan site. 4-15% gradient SDS protein gel (BioRad) of purified WT and NG monoclonal anti-TT IgG D2 under non-reduced (IgG) and reduced (HC and LC) conditions. The size-shift caused by the presence of VDGs is visible. The size was determined using the PageRulerTM Plus Prestained Protein Ladder (Thermo Fisher Scientific). (**B**) LC-MS Fc-peptide glycan analysis of WT, HCWT, LCWT and NG 7E4 and (**C**) 3F3 mAb variants. The amount of galactosylation (Gal), sialylation (Sial), bisection (Bis) and fucosylation (Fuc) per N-glycan is shown. (**D**) LC-MS Fc-peptide glycan analysis of WT and NG RGY mutants. The amount of galactosylation (Gal), sialylation (Sial), bisection (Bis) and fucosylation (Fuc) per N-glycan is shown.

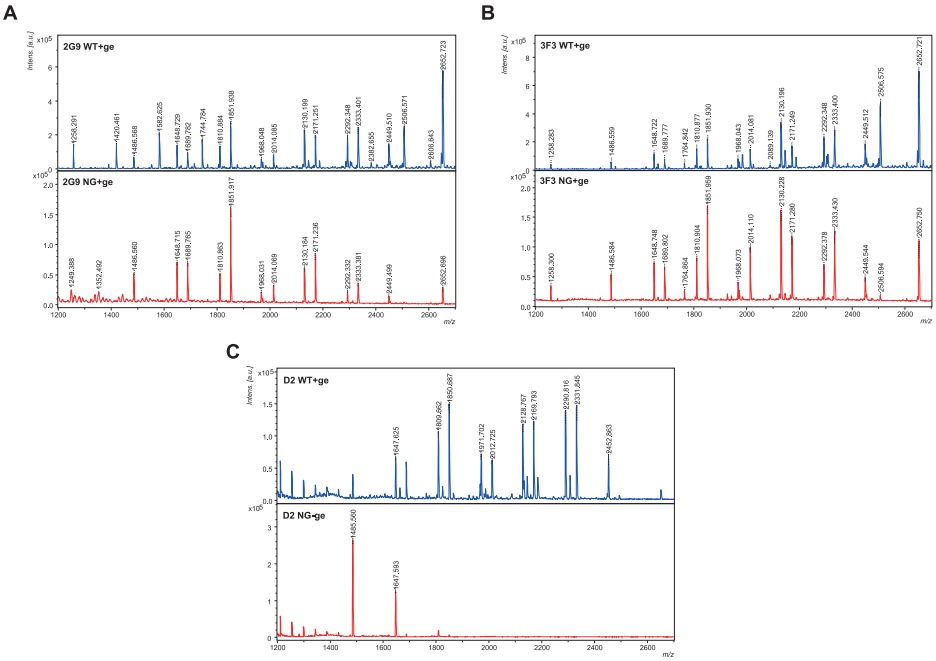

Figure S2. MALDI-TOF MS analysis of released and stabilized VD and Fc glycans from WT and NG 2G9, 3F3 and D2 mAbs. The m/z of the glycan peaks are depicted. Blue square: *N*-acetylglucosamine (GlcNAc), green circle: mannose, yellow circle: galactose, red triangle: fucose, purple diamond: α 2,6-linked *N*-acetylneuraminic acid (sialic acid).

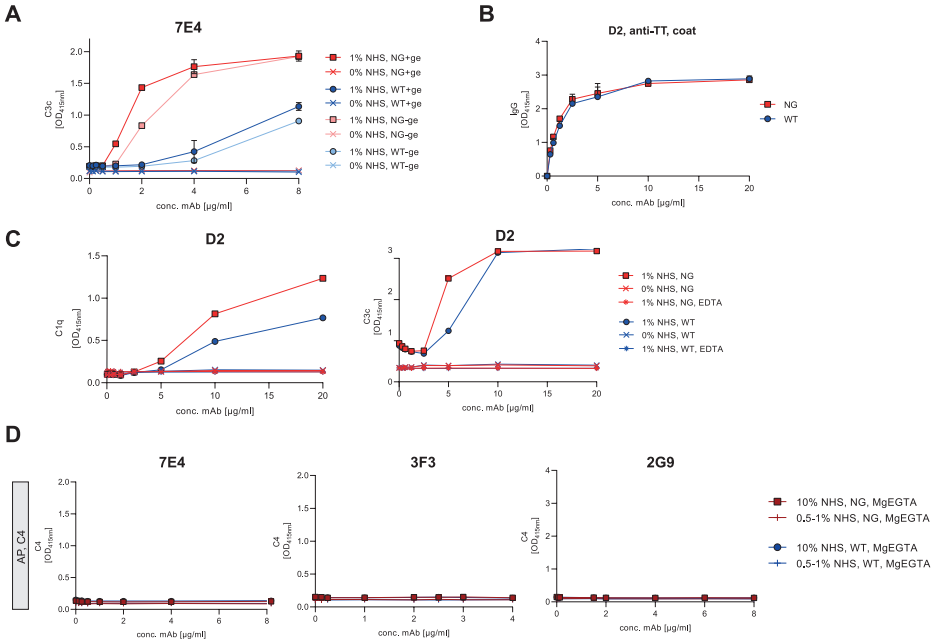

Figure S3. Complement pathway activation of mAbs. (**A**) Classical pathway activation. C3c deposition on WT and NG +/-ge 7E4 mAbs (0 to 8 µg/ml) after adding 0% or 1% NHS in gelatin veronal buffer containing Ca^{2+} and Mg^{2+} (GVB++). Each data point represents the mean of two technical replicates. (**B**) Detection of WT and NG mAb D2 (a-TT) binding to ELISA plates. Each data point represents the mean of two technical replicates. (**C**) Classical pathway activation. C1q and C3c deposition on WT and NG mAb D2 after adding 0% or 1% NHS in GVB++. (**D**) C4 deposition on WT and NG mAb (7E4, 3F3 and 2G9) after adding alternative pathway buffer (1% or 10% NHS in Mg-EGTA).

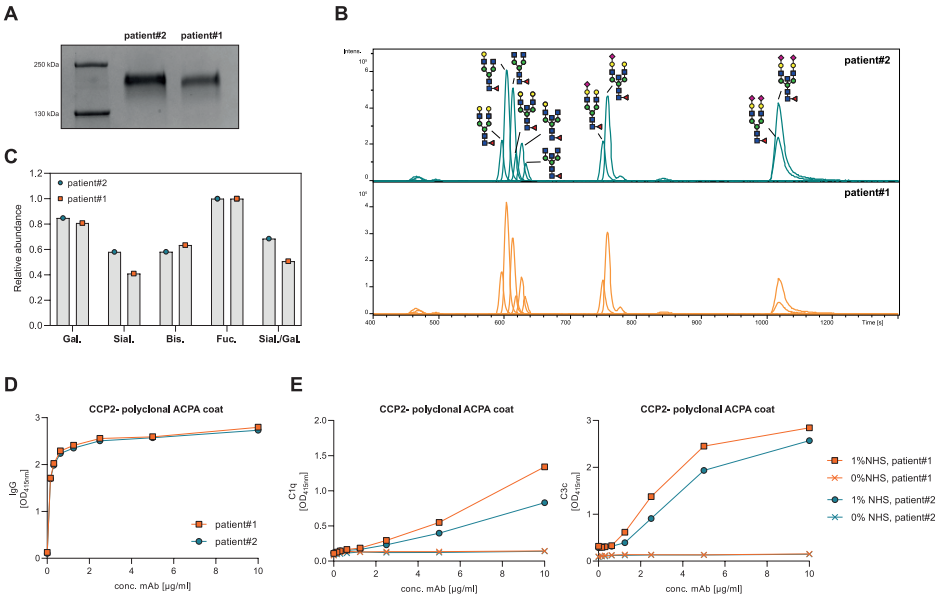

Figure S4. Classical complement pathway activation of polyclonal ACPA IgG with different quantities of VDGs isolated from RA patient serum samples. (**A**) 4 to 15% gradient SDS protein gel (BioRad) of patient isolated polyclonal ACPA IgG. The size-shift between the polyclonal ACPA IgG from patient #1 vs. patient #2 caused by the presence of different quantities of VDGs is visible. The size was determined using the PageRuler™ Plus Prestained Protein Ladder (Thermo Fisher Scientific). (**B**) LC-chromatogram of released and stabilized VD and Fc glycans from patient#1 and #2. The schematic N-glycan composition per elution peak is depicted. Blue square: *N*-acetylglucosamine (GlcNAc), green circle: mannose, yellow circle: galactose, red triangle: fucose, purple diamond: α 2,6-linked *N*-acetylneuraminic acid (sialic acid). (**C**) Amount of galactosylation (Gal), sialylation (Sial), bisection (Bis) and fucosylation (Fuc) per N-glycan (VD and Fc glycans) based on the quantified LC-MS results. (**D**) Detection of polyclonal ACPA IgG (0 to 10 µg/ml) binding to CCP2-coated ELISA plate. (**E**) Classical pathway activation. C1q and C3c deposition on polyclonal ACPA IgG (0 to 10 µg/ml) from patient #1 and #2 with different VDG quantities after adding 0% or 0.5% NHS in GVB++.

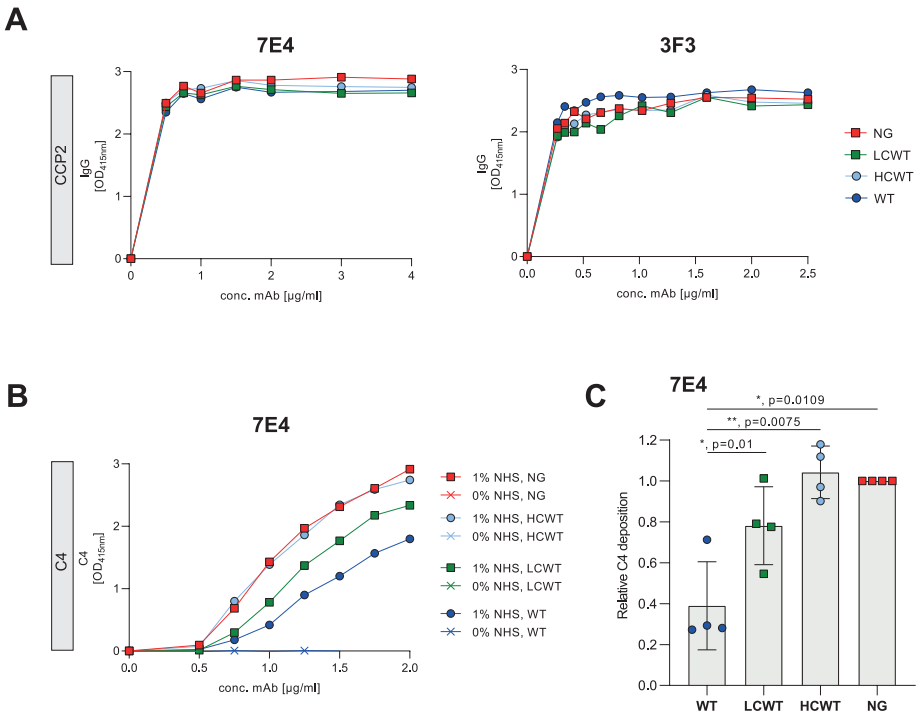

Figure S5. CCP2-binding (3F3 and 7E4) and C4 deposition (7E4) of monoclonal ACPA IgG with different quantities of VDGs in heavy and light chain. (**A**) Detection of WT, HCWT, LCWT and NG binding to CCP2-coated ELISA plate for mAb 7E4 and mAb 3F3. (**B**) Classical pathway activation. C4 deposition on WT, HCWT, LCWT and NG 7E4 after adding 0% or 1% NHS in GVB++. (**C**) Relative C4 deposition of WT, HCWT, LCWT mAb 7E4 (2 µg/ml) compared to its NG counterpart. Each binding experiment was repeated 4 times and each dot represents one independent experiment. The respective p-values are depicted: ns $p > 0.05$, *$p \leq 0.05$, **$p \leq 0.01$, ***$p \leq 0.001$ or ****$p \leq 0.0001$.

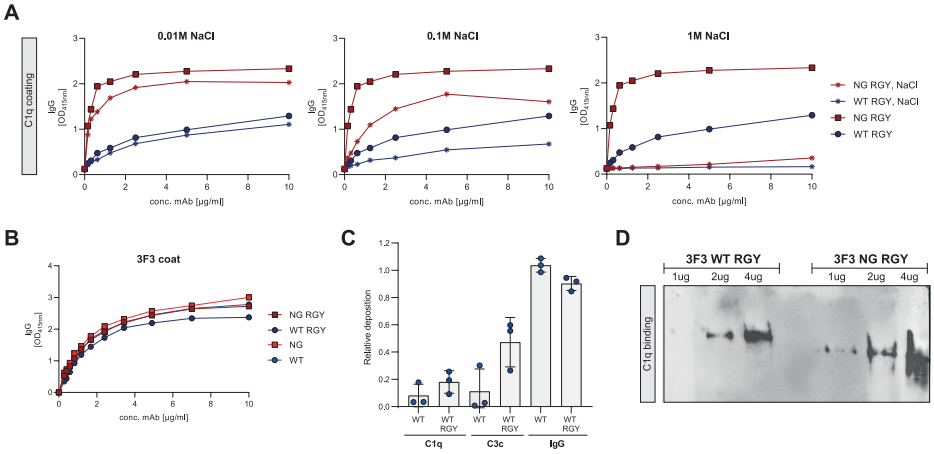

Figure S6. C1q binding of 3F3 RGY mutants. (**A**) Detection of WT, NG, WT RGY and NG RGY 3F3 mAb binding to C1q-coated ELISA plate after incubation with 0.01 M, 0.1 M or 1 M NaCl to specifically disrupt the C1q head domain interactions. (**B**) Detection of monomeric WT and NG and WT RGY and NG RGY 3F3 mAb (0 to 10 µg/ml) binding to CCP2-coated ELISA plate. (**C**) Relative C1q, C3c and IgG deposition of WT vs. WT RGY. Each experiment was repeated 3 times and each dot represents one independent experiment. (**D**) Western blot of native 7% TRIS-acetate gel after incubation in 0.05% SDS. Binding to recombinantly added human native C1q (CompTech) was detected using rabbit anti-C1q (DAKO) and HRP-labelled goat anti-rabbit (DAKO) detection antibodies.